

9

Outstanding Questions and Future Prospects

In this chapter we shall describe a few of the outstanding questions in both nuclear and particle physics and future prospects for their solution. The list is by no means exhaustive (particularly for nuclear physics, which has a very wide range of applications) and concentrates mainly on those areas touched on in earlier chapters. The examples should be sufficient to show that nuclear and particle physics remain exciting and vibrant subjects with many interesting phenomena being discovered and questions awaiting explanations.

9.1 Particle Physics

Unlike nuclear physics, particle physics does have a comprehensive theory, but although the standard model is very successful at explaining a wide range of phenomena, there are still questions that remain to be answered and some hints from experiments of phenomena that lie outside the model, for example neutrino oscillations and the possibility of lepton number violation. In addition, the success of the standard model has spurred physicists to construct theories that incorporate the strong interaction, and even in some cases gravity, in wider unification schemes. A full discussion of these topics is beyond the scope of this book, but in this chapter we will briefly review some of these questions and also look at the rapidly growing field of particle astrophysics.

9.1.1 The Higgs boson

The Higgs boson is an electrically neutral spin-0 boson whose existence is predicted by the unified electroweak theory, but which has not yet been observed.

It is required because of a fundamental symmetry associated with theories in which the force carriers are spin-1 bosons. This symmetry is called gauge invariance and has been mentioned in previous chapters. Gauge invariance can be shown to require that the spin-1 ‘gauge bosons’ have zero masses if they are the only bosons in the theory. This is acceptable for QED and QCD, since the gauge bosons are photons and gluons and they do indeed have zero masses. Gauge invariance also plays a crucial role in the unified electroweak theory, where it is needed to ensure the cancellation of the divergences that occur in individual higher-order Feynman diagrams. In this case the result is even stronger and it can be shown that gauge invariance requires that the *all* the fundamental particles – quarks, leptons and gauge bosons – have zero masses if gauge bosons are the only bosons in the theory. This prediction is clearly in contradiction with experiment, because the W and Z bosons have masses about 80–90 times that of the nucleon. This problem, known as the *origin of mass*, is overcome by assuming that the various particles interact with a new field, called the *Higgs field*, whose existence can be shown to allow the gauge bosons to acquire masses without violating the gauge invariance of the interaction.¹ The ‘price’ of this is that there must exist electrically neutral quanta associated with the Higgs field, called *Higgs bosons*, in the same way that there are quanta associated with the electromagnetic field, i.e. photons.

We saw in Chapter 3, that there is evidence that neutrinos, originally assumed to have zero masses in the standard model, are in fact not massless. The Higgs mechanism can also, in principle, be invoked to generate masses for neutrinos. However, it would be natural to expect that such masses would then be roughly the same size as the masses generated for the gauge bosons and we have seen that this is clearly not the case. This problem can only be avoided if the coupling of the neutrinos to the Higgs field is at least 12 orders of magnitude smaller than that of the coupling of the top quark. Many physicists reject such an explanation as implausible and alternative mechanisms have been suggested for generating very small neutrino masses. All have problems of their own and at present none is universally accepted. Experiments currently being planned should help resolve the matter.

The existence of the Higgs boson is the most important prediction of the standard model that has not been verified by experiment, and searches for it are of the highest priority. A problem in designing suitable experiments is that its mass is not predicted by the theory. However, its couplings to other particles *are* predicted and are essentially proportional to the masses of the particles to which it couples. The Higgs boson therefore couples very weakly to light particles like neutrinos, electrons, muons and u , d , s quarks; and much more strongly to heavy particles like W^\pm and Z^0 bosons, and presumably b and t quarks. Hence attempts to produce Higgs bosons are made more difficult by the need to first produce the very heavy particles to which they couple.

¹This process is called ‘spontaneous symmetry breaking’ and was mentioned in Chapter 6.

The failure to observe Higgs bosons in present experiments leads to limits on their mass. The best results come from the Large Electron–Positron (LEP) accelerator at CERN. This machine (which is no longer operational) had a maximum energy of 208 GeV, which is enough to produce Higgs bosons with masses up to almost $120 \text{ GeV}/c^2$ in the reaction

$$e^+ + e^- \rightarrow H^0 + Z^0, \quad (9.1)$$

which is expected to occur by the dominant mechanism of Figure 9.1.

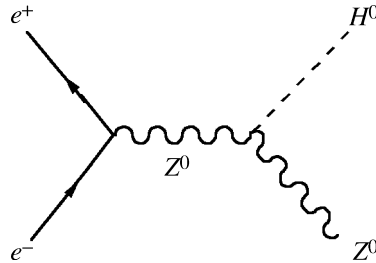


Figure 9.1 Dominant mechanism for Higgs boson production in e^+e^- annihilation

Attempts were made to detect Higgs bosons by their decays to $b\bar{b}$ pairs, where the quarks would be observed as jets containing short-lived hadrons with non-zero beauty. The results were tantalizing. By the time LEP closed down in November 2000 to make way for another project, it had shown that no Higgs bosons existed with a mass less than $113.5 \text{ GeV}/c^2$; and some evidence had been obtained for the existence of a Higgs boson with a mass of $115 \text{ GeV}/c^2$. This is very close to the upper limit of masses that were accessible by LEP, but because the Higgs boson would have a width, its mass distribution would extend down to lower energies and would give a signal. Unfortunately, while this signal was statistically likely to be a genuine result rather than a statistical fluctuation, the latter cannot be completely ruled out.

Future investigations will involve the use of new accelerators currently under construction, particularly the LHC proton–proton collider mentioned in Chapter 4. (One of the detectors at the LHC, ATLAS was shown in Figure 4.19.) This will enable searches to be made for Higgs bosons with masses up to $1 \text{ TeV}/c^2$ via reactions of the type

$$p + p \rightarrow H^0 + X, \quad (9.2)$$

where X is any state allowed by the conservation laws. The mechanism for this reaction is the weak interaction between the constituent quarks of the protons, an example of which is shown in Figure 9.2, where the other quarks in the protons are spectators, as usual.

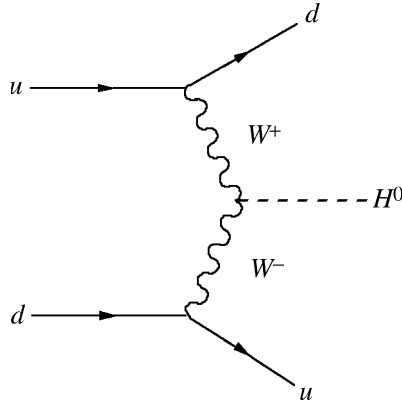


Figure 9.2 An example of a process that can produce Higgs bosons in pp collisions

The reaction in Equation (9.2) will take place against a large background of strong interaction processes and the method of detecting it will depend on the actual Higgs boson mass. If $M_H > 2M_W$, then the Higgs boson can decay to a pair of W -mesons or Z^0 -mesons, which themselves decay. For example, from the leptonic decay of the Z^0 s, we could have overall the reaction

$$H^0 \rightarrow \ell^+ + \ell^- + \ell^+ + \ell^-, \quad (\ell = e, \mu). \quad (9.3)$$

This would enable the mass range $200 \text{ GeV}/c^2 \leq M_H \leq 500 \text{ GeV}/c^2$ to be explored. However, the branching ratios are such that only a few per cent of decays will have such a distinctive signal and other decays modes will also have to be explored. For lower masses such that $M_H < 2M_W$ where these decays are energetically forbidden, one might think of looking for decays to fermion–antifermion pairs. Because the Higgs boson preferentially couples to heavy particles, the dominant decay of this type will be $H^0 \rightarrow b + \bar{b}$ with accompanying jets. This was the method used in the LEP experiments referred to above. Unfortunately, it is very difficult to distinguish these jets from those produced by other means. Rarer decay modes, but with more distinctive signals, will have to be sought, such as $H^0 \rightarrow \gamma + \gamma$, which in the standard model has a branching ratio of about 10^{-3} .

All the above is based on the standard model with a single neutral Higgs boson, but we will see in Section 9.1.3 that realistic extensions of the standard model require several Higgs bosons, not all of which are electrically neutral. Experimental investigations of the Higgs sector will undoubtedly play a central role in the future of particle physics for many years to come.

9.1.2 Grand unification

Whether or not the Higgs boson exists is the most pressing unanswered question of the standard model but, even if it is found with its predicted properties, this is not

the end of the story, because one of the goals of particle theory is to have a single universal theory that explains all the phenomena of the subject. Since we already have a unified theory for the weak and electromagnetic interactions, the next logical step is to try to include the strong interaction. Attempts to do this are called *grand unified theories* (GUTs).

We have seen that unification of the weak and electromagnetic interactions does not manifest itself until energies of the order of the W and Z masses. To get some idea of the energy scale of a grand unified theory, we show in Figure 9.3 the couplings²

$$g \equiv 2\sqrt{2}g_W, \quad g' \equiv 2\sqrt{2}g_Z \quad (9.4)$$

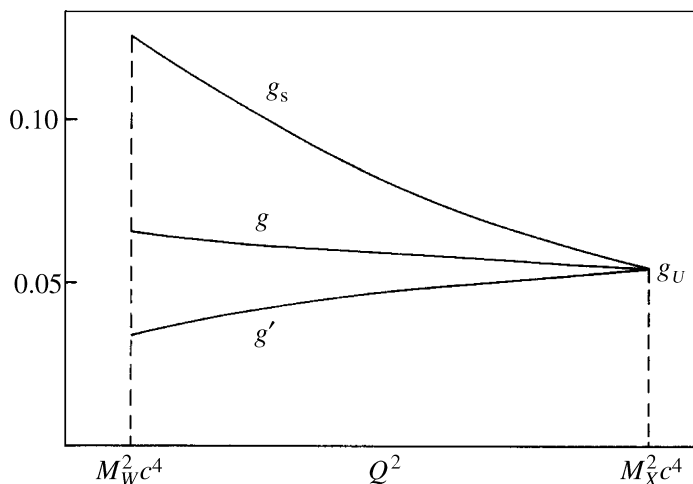


Figure 9.3 Idealized behaviour of the strong and electroweak coupling as functions of the squared energy-momentum transfer Q^2 in a simple grand unified theory; g_U is the unification coupling

and the strong coupling g_s (this is related to α_s by $\alpha_s = g_s^2/4\pi$) as functions of Q^2 , the squared energy-momentum transfer in a typical GUT. A naïve extrapolation in Q^2 (using, for example, Equation (5.11)) from the region where these couplings are presently known suggests that they become approximately equal to a single value g_U at the enormous energy $Q^2 = M_X^2 c^4$, where M_X , the so-called *unification mass*, is of the order of 10^{15} GeV/ c^2 . In practice, which couplings to extrapolate depends on which version of GUT one considers, but if the extrapolation is done accurately the three curves actually fail to meet at a point by an amount that cannot be explained by uncertainties in the models.

²Recall that the electromagnetic coupling e is related to these couplings by the unification condition Equation (6.71).

There are many potential grand unified theories, but the simplest incorporates the known quarks and leptons into common families. For example, one way is to put the three coloured d -quarks and the doublet $(e^+, \bar{\nu}_e)$ (strictly their right-handed components) into a common family, i.e.

$$(d_r, d_b, d_g, e^+, \bar{\nu}_e). \quad (9.5)$$

The fundamental vertex interactions allowed in this model are shown in Figure 9.4.

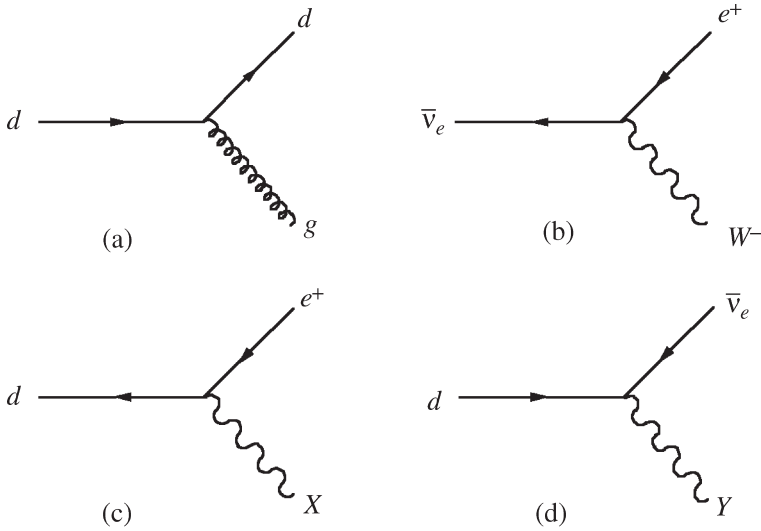


Figure 9.4 Fundamental vertices that can occur for the multiplet of particles in Equation (9.5)

In addition to the known QCD interaction in (a) and the electroweak interaction in (b), there are two new interactions represented by (c) and (d) involving the emission or absorption of two new gauge bosons X and Y with electric charges $-\frac{4}{3}$ and $-\frac{1}{3}$, respectively, and masses of the order of M_X . In this theory all the processes of Figure 9.4 are characterized by a single GUT coupling given by

$$\alpha_U \equiv \frac{g_U^2}{4\pi} \approx \frac{1}{42}, \quad (9.6)$$

which is found by extrapolating the known coupling of the standard model to the energy $M_X c^2$.

This simple model has a number of attractive features. For example, it can be shown that the sum of the electric charges of all the particles in a given multiplet is zero. So, using the multiplet $(d_r, d_b, d_g, e^+, \bar{\nu}_e)$, it follows that

$$3q_d + e = 0, \quad (9.7)$$

where q_d is the charge of the down quark. Thus $q_d = -e/3$ and the fractional charges of the quarks is seen to originate in the fact that they exist in three colour states. By a similar argument, the up quark has charge $q_u = 2e/3$ and so with the usual quark assignment $p = uud$, the proton charge is given by

$$q_p = 2q_u + q_d = e. \tag{9.8}$$

Thus, we also have an explanation of the long-standing puzzle of why the proton and positron have precisely the same electric charge.

GUTs make a number of predictions that can be tested at presently accessible energies. For example, if the three curves of Figure 9.3 really did meet at a point, then the three low-energy couplings of the standard model would be expressible in terms of the two parameters α_U and M_X . This could be used to predict one of the former, or equivalently the weak mixing angle θ_W . The result is $\sin^2 \theta_W = 0.214 \pm 0.004$, which is close to the measured value of 0.2313 ± 0.0003 , although not strictly compatible with it. (This is true even if the effect of the Higgs boson is taken into account when evaluating the evolution of the coupling constants.)

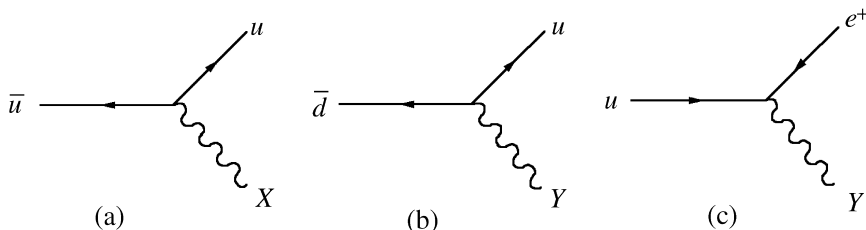


Figure 9.5 The three fundamental vertices predicted by the simplest GUT involving the gauge bosons X and Y (these are in addition to those shown in Figure 9.4)

In addition to the interactions of the X and Y bosons shown in Figure 9.4, there are a number of other possible vertices, which are shown in Figure 9.5. (There is also another set where particles are changed to antiparticles.) A consequence of these interactions and those of Figure 9.4(c) and (d) is the possibility of reactions that conserve neither baryon nor lepton numbers. The most striking prediction of this type is that the proton would be unstable, with decay modes such as $p \rightarrow \pi^0 + e^+$ and $p \rightarrow \pi^+ + \bar{\nu}_e$. Examples of Feynman diagrams for these decays are shown in Figure 9.6 and are constructed by combining the vertices of Figure 9.4 and 9.5. In all such processes, although lepton number L and baryon number B are not conserved, the combination

$$R \equiv B - \sum_{\ell} L_{\ell} \quad (\ell = e, \mu, \tau) \tag{9.9}$$

is conserved.

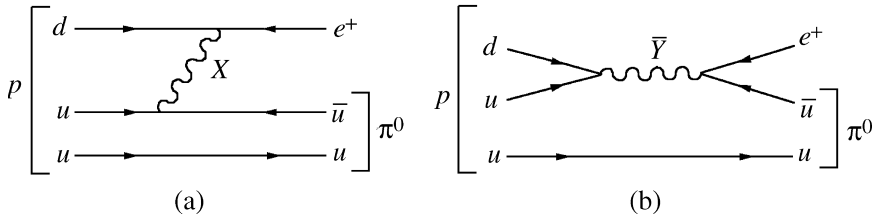


Figure 9.6 Examples of processes that contribute to the proton decay mode $p \rightarrow \pi^0 + e^+$

Since the masses of the X and Y bosons are far larger than the quarks and leptons, we can use the zero-range approximation to estimate the lifetime of proton decay. In this approximation, and by analogy with the lifetime for the muon Equation (7.62), we have for the proton lifetime

$$\tau_p \approx \frac{(M_X c^2)^4}{g_U^4 (M_p c^2)^5}. \quad (9.10)$$

Taking account of reasonable uncertainties on g_U and M_X , this gives

$$\tau_p \approx 10^{30 \pm 1} \text{ years}. \quad (9.11)$$

Proton decay via these modes has been looked for experimentally. The most extensive search has been made using the Kamiokande detector described in Chapter 4. To date no events have been observed and this enables a lower limit to be put on the proton lifetime of about 10^{32} years, which rules out the simplest version of a grand unified theory. However, there are other, more complicated, versions that still cannot be completely ruled out by present experiments. Some of these incorporate the idea of *supersymmetry* which is described below.

Finally, GUTs may offer an explanation for the very small neutrino masses observed in the oscillation experiments discussed in Chapter 3. In Section 6.3 we discussed the possibility that the neutrino was its own antiparticle (a so-called Majorana neutrino). In GUTs the right-handed neutrino states are predicted to be very massive (of order 10^{17} GeV/ c^2) and mix with the massless left-handed neutrinos of the standard model to give physical neutrinos with masses

$$m_\nu \sim m_L^2 / M_X, \quad (9.12)$$

where m_L is the typical mass of a charged lepton or quark.

9.1.3 Supersymmetry

One of the problems with GUTs is that if there are new particles associated with the unification energy scale, then they would have to be included as additional

contributions in the higher-order calculations in the electroweak theory, for example for the mass of the W -boson. These contributions would upset the delicate cancellations that ensure finite results from higher-order diagrams in the standard model, unless there were some way of cancelling these new contributions. Supersymmetry (SUSY) does exactly this.

Supersymmetry is the proposal that every known elementary particle has a partner, called a *superpartner*, which is identical to it all respects except its spin. Spin- $\frac{1}{2}$ particles have spin-0 superpartners and spin-1 particles have spin- $\frac{1}{2}$ superpartners. To distinguish between a spin- $\frac{1}{2}$ particle and its superpartner, an ‘s’ is attached to the front of its name in the latter case. Thus, for example, a spin- $\frac{1}{2}$ electron has a spin-0 *selectron* as its superpartner. The full set of elementary particles and their superpartners in the simplest SUSY model (the so-called Minimal Supersymmetric Standard Model – MSSM) is shown in Table 9.1. (This is actually a simplification because even the simplest SUSY requires a number of different Higgs bosons, not all electrically neutral.)

Table 9.1 The particles of the MSSM and their superpartners

| Particle | Symbol | Spin | Superparticle | Symbol | Spin |
|-------------|----------|---------------|---------------|------------------|---------------|
| Quark | q | $\frac{1}{2}$ | Squark | \tilde{q} | 0 |
| Electron | e | $\frac{1}{2}$ | Selectron | \tilde{e} | 0 |
| Muon | μ | $\frac{1}{2}$ | Smuon | $\tilde{\mu}$ | 0 |
| Tauon | τ | $\frac{1}{2}$ | Stauon | $\tilde{\tau}$ | 0 |
| W -boson | W | 1 | Wino | \tilde{W} | $\frac{1}{2}$ |
| Z -boson | Z | 1 | Zino | \tilde{Z} | $\frac{1}{2}$ |
| Photon | γ | 1 | Photino | $\tilde{\gamma}$ | $\frac{1}{2}$ |
| Gluon | g | 1 | Gluino | \tilde{g} | $\frac{1}{2}$ |
| Higgs boson | H | 0 | Higgsino | \tilde{H} | $\frac{1}{2}$ |

If the symmetry were exact then a particle and its superparticle would have equal masses. This is clearly not the case or such states would have already been found. So supersymmetry is at best an approximate symmetry of nature. Nevertheless, even in an approximate symmetry, the couplings of the two states are equal and opposite, thereby ensuring the required cancellation, providing their masses are not too large. In practice, it is usually assumed in GUTs that incorporate supersymmetry that the masses of the superparticles are of the same order as the masses of the W and Z bosons. With the inclusion of superparticles, the evolution of the coupling constants of the standard model as functions of Q^2 changes slightly and when extrapolated they meet very close to a single point. The unification mass is increased somewhat to about 10^{16} GeV/ c^2 , while the value of g_U remains roughly constant. Thus the predicted lifetime of the proton is increased to about $10^{32} - 10^{33}$ years, conveniently beyond the ‘reach’ of current experiments. At the same time, the value of the weak mixing angle is brought into almost exact agreement with the measured value. Whether this is simply a coincidence or not is unclear.

To verify supersymmetry it will of course be essential to detect the superparticles and that will not be easy. For example, the virtual exchange of superparticles could contribute to the deviation of the muon magnetic dipole moment from its Dirac value, although it would be difficult to separate these contributions from other corrections. To date, activity has concentrated on the direct detection of superparticles in reactions. In the simplest version of a SUSY theory, superparticles are produced in pairs (like leptons or strange particles in strong interactions, i.e. associated production) so that the decay of a superparticle must have at least one superparticle in the final state and the lightest such particle will necessarily be stable. Most versions of SUSY theories assume that the lightest particle will be a *neutralino* $\tilde{\chi}_0$, which is the name given to a mixture of the photino, the higgsino and the zino, the three spin- $\frac{1}{2}$ superparticles that interact purely by the electroweak interaction. If this is the case, a possible reaction that could be studied is

$$e^+ + e^- \rightarrow \tilde{e}^+ + \tilde{e}^-, \quad (9.13)$$

followed by the decays

$$\tilde{e}^\pm \rightarrow e^\pm + \tilde{\chi}^0, \quad (9.14)$$

giving overall

$$e^+ + e^- \rightarrow e^+ + e^- + \tilde{\chi}_0 + \tilde{\chi}_0. \quad (9.15)$$

The cross-section for Equation (9.13) is predicted to be comparable to that for producing pairs of ordinary charged particles. As the neutralinos only have weak interactions they will be undetectable in practice and so the reaction would be characterized by e^+e^- pairs in the final state with only a fraction (typically 50 per cent) of the initial energy and not emerging ‘back-to-back’ (because it is not a two-body reaction). This and many other reactions have been studied, mainly in experiments at LEP, but to date no evidence for the existence of superparticles has been found. The null results have enabled lower limits to be set on the masses of neutralinos and sleptons of various flavours in the range, 40 – 100 GeV/ c^2 . This is not very useful in practice, as the masses are believed to be of the order of the W and Z masses. Much larger lower limits for the masses of gluinos and squarks have been obtained in experiments using the CDF detector that was described in Chapter 4 (see Figure 4.18). The search for supersymmetric particles will be a major activity of detectors at the LHC accelerator currently under construction at CERN.³

Undeterred by the lack of immediate success of supersymmetry, some bold physicists have attempted to incorporate gravity into even larger unified schemes.

³For a review of the current state of experimental searches for superparticles see, for example, Ei04.

The problems here are formidable, not least of which is that the divergences encountered in trying to quantize gravity are far more severe than those in either QCD or the electroweak theory and there is at present no successful ‘stand-alone’ quantum theory of gravity analogous to the former two. The theories that have been proposed that include gravity invariably replace the idea of point-like elementary particles with tiny quantized *strings* as a device to reduce these technical problems and are formulated in many more dimensions (usually 10 or 11) than we observe in nature. More recently, even strings have been superseded by theories based on mathematical objects called membranes, or simply *branes*. The problem with these theories, leaving aside their formidable mathematical complexity, is that they apply at an energy scale where gravitational effects are comparable to those of the gauge interactions, i.e. at energies defined by the so-called *Planck* mass M_P , which is given by

$$M_P = \left(\frac{\hbar c}{G} \right)^{1/2} = 1.2 \times 10^{19} \text{ GeV}/c^2, \quad (9.16)$$

where G is the gravitational constant.⁴ This energy is so large that it is difficult to think of a way that the theories could be tested at currently accessible energies, or even indeed at energies accessible in the conceivable future. Their appeal at present is, therefore, the mathematical beauty and ‘naturalness’ that their sponsors claim for them. Needless to say, experimentalists will remain sceptical until definite experimental tests can be suggested and carried out.

9.1.4 Particle astrophysics

Particle physics and astrophysics interact in an increasing number of areas and the resulting field of particle astrophysics is a rapidly expanding one. The interactions are particularly important in the field of cosmology where, for example, the detection of neutrinos can provide unique cosmological information. Another reason is because the conditions in the early Universe implied by standard cosmological theories (the big bang model) can only be approached, however remotely, in high-energy particle collisions. At the same time, these conditions occurred at energies that are relevant to the grand unified and SUSY theories of particle physics and so offer a possibility of testing the predictions of such theories. This is important because, as mentioned above, it is difficult to see other ways of testing such predictions. For reasons of space, we will discuss just three examples of particle astrophysics. We will return to the question of conditions in the early universe in Section 9.2.2.

⁴This implies that strings have dimensions of order $\ell_p \sim \hbar/M_P c = 1.6 \times 10^{-35}$ m.

Neutrino astrophysics

We have seen in Chapter 3 that cosmic rays and emissions from the Sun are important sources of information about neutrinos and have led us to revise the view that neutrinos are strictly massless, as is assumed in the standard model. At the same time, there is considerable interest in studying ultra high-energy neutrinos as a potential source of information about galactic and extra-galactic objects and hence cosmology in general.

One of the first neutrino astrophysics experiments was the observation of neutrinos from a supernova. Supernovas are very rare events where a star literally explodes with a massive output of energy over a very short timescale measured in seconds. The mechanism for this (briefly) is as follows. If a star has a mass greater than about 11 solar masses, it can evolve through all stages of fusion, ending in a core of iron surrounded by shells of lighter elements. Because energy cannot be released by the thermonuclear fusion of iron, the core will start to contract under gravity. Initially this is resisted by the pressure of the dense gas of degenerate electrons in the core (*electron degeneracy pressure*), but as more of the outer core is burned and more iron deposited in the core, the resulting rise in temperature makes the electrons become increasingly relativistic. When the core mass reaches about 1.4 solar masses (the so-called *Chandrasekhar limit*), the electrons become ultra relativistic and they can no longer support the core. At this point the star is on the brink of a catastrophic collapse.

The physical reactions that lead to this are as follows. Firstly, photodisintegration of iron (and other nuclei) takes place,



which further heats the core and enables the photodisintegration of the helium produced, i.e.



As the core continues to collapse, the energy of the electrons present increases to a point where the weak interaction



becomes possible and eventually the hadronic matter of the star is predominantly neutrons. This stage is therefore called a *neutron star*. The collapse ceases when the gravitational pressure is balanced by the neutron degeneracy pressure. At this point the radius of the star is typically just a few kilometres. The termination of the collapse is very sudden and as a result the core material produces a shock wave that travels outwards through the collapsing outer material, leading to a supernova (actually a so-called Type II supernova). Initially there is an intense burst of ν_e

with energies of a few MeV from the reaction of Equation (9.19). This lasts for a few milliseconds because the core rapidly becomes opaque even to neutrinos and after this the core material enters a phase where all its constituents (nucleons, electrons, positrons and neutrinos) are in thermal equilibrium. In particular, all flavours of neutrino are present via the reactions

$$\gamma \rightleftharpoons e^+e^- \rightleftharpoons \nu_\ell\bar{\nu}_\ell, \quad (\ell = e, \mu, \tau) \quad (9.20)$$

and these will eventually diffuse out of the collapsed core and escape. Neutrinos of all flavours, with average energies of about 15 MeV, will be emitted in all directions over a period of 0.1–10 s. Taken together, the neutrinos account for about 99 per cent of the total energy released in a supernova. Despite this, the output in the optical region is sufficient to produce a spectacular visual effect.

The first experiments to detect neutrinos from a supernova were an earlier version of the Kamiokande experiment described in Chapter 3 and the IMB collaboration, which also used a water Čerenkov detector. Both had been constructed to search for proton decay as predicted by GUTs, but by good fortune both detectors were ‘live’ in 1987 at the time of a spectacular supernova explosion (now named SN1987A) and both detected a small number of antineutrino events. The data are shown in Figure 9.7. The Kamiokande experiment detected 12 $\bar{\nu}_e$ events and the IMB experiment eight events, both over a time interval of approximately 10 s and with energies in the range 0–40 MeV. These values are consistent with the estimates for the neutrinos that would have been produced by the reaction in Equation (9.20) and then diffused from the supernova after the initial pulse.

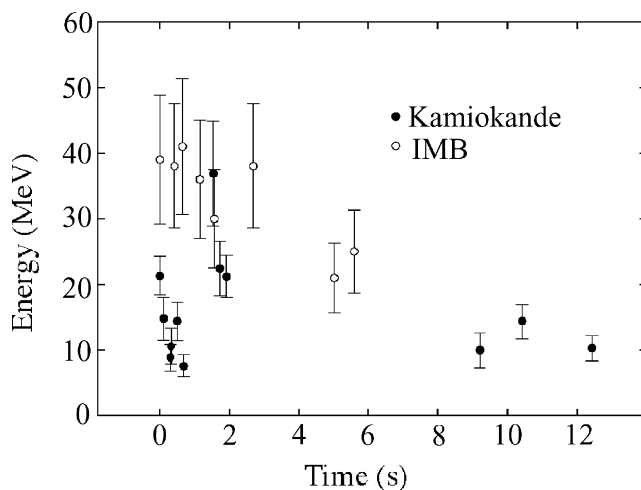


Figure 9.7 Data for neutrinos from SN1987A detected in the Kamiokande and IMB experiments: the threshold for detecting neutrinos in the experiments are 6 MeV (Kamiokande) and 20 MeV (IMB) -- in each case the first neutrino detected is assigned the time zero

The data can be used to make an estimate of the neutrino mass as follows. The time of arrival on Earth of a neutrino i is given by

$$t_i = t_0 + \left(\frac{L}{c}\right) \left[1 + \frac{m^2 c^4}{2E_i^2}\right], \quad (9.21)$$

where t_0 is the time of emission from the supernova and (m, E_i) are the mass and total energy of the neutrino. Thus

$$(\Delta t)_{ij} \equiv t_i - t_j = \frac{L m^2 c^4}{2c} \left[\frac{1}{E_i^2} - \frac{1}{E_j^2} \right]. \quad (9.22)$$

Using data for pairs of neutrinos, Equation (9.22) leads to the result

$$m_{\bar{\nu}_e} \leq 20 \text{ eV}, \quad (9.23)$$

which, although larger than the value from tritium decay, is still a remarkable measurement.

The neutrinos from SN1987A were of low energy, but there is also a great interest in detecting ultra high-energy neutrinos. For example, it is known that there exist point sources of γ -rays with energies in the TeV range, many of which have their origin within so-called *active galactic nuclei*. It is an open question whether this implies the existence of point sources of neutrinos with similar energies. The neutrinos to be detected would be those travelling upwards through the Earth, as the signal from downward travelling particles would be swamped by neutrinos produced via pion decay in the atmosphere above the detector. Like all weak interactions the intrinsic rate would be very low, especially so for such high-energy events, but this is partially compensated by the fact that the ν -nucleon cross-section increases with energy, as we showed in Chapter 6.

To detect neutrinos in the TeV energy range using the Čerenkov effect in water requires huge volumes, orders-of-magnitude larger than used in the Super-Kamiokande detector. An ingenious solution to this problem is to use the vast quantities of water available in liquid form in the oceans, or frozen in the form of ice at the South Pole, and several experiments have been built, or are being built, using these sources. The largest so far is the Antarctic Muon and Neutrino Detector Array (AMANDA) which is sited at the geographical South Pole. A schematic diagram of this detector is shown in Figure 9.8.

The detector consists of strings of optical modules containing photomultiplier tubes that convert the Čerenkov radiation to electrical signals. The enlarged inset in Figure 9.8 shows the details of an optical module. They are located in the ice at great depths by using a novel hot-water boring device. The ice then refreezes around them. In the first phase of the experiment in 1993/94 (AMANDA-A) four detector strings were located at depths of between 800 and 1000 m. The ice at

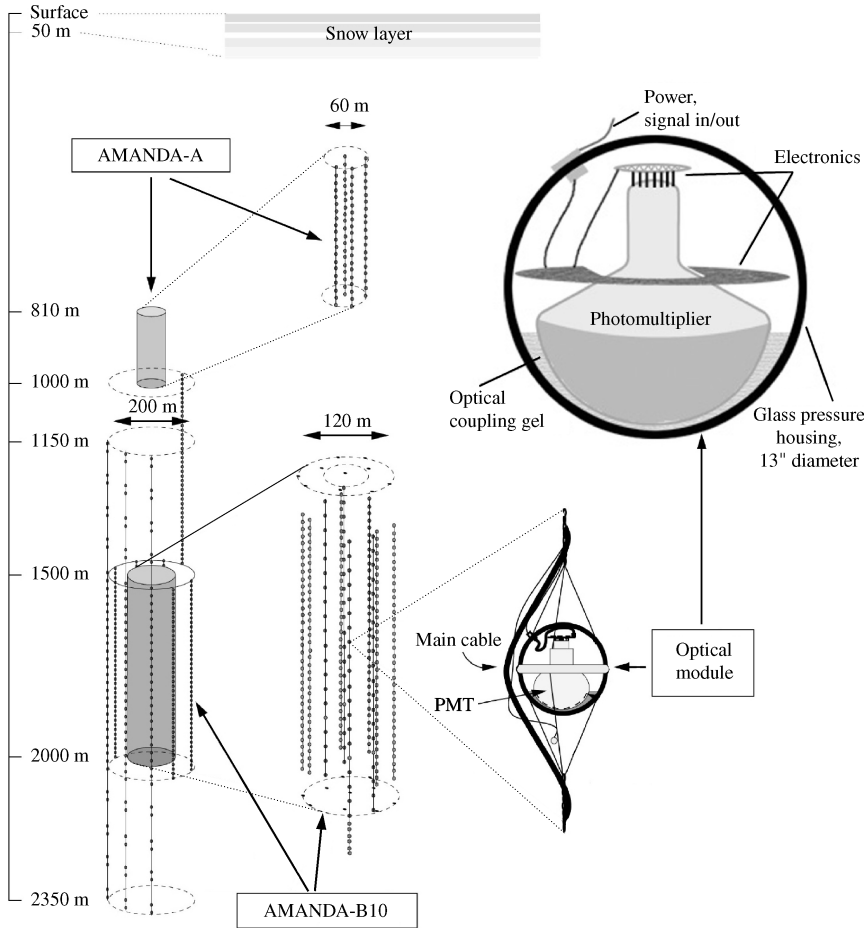


Figure 9.8 A schematic diagram of the AMANDA neutrino detector

these depths is filled with air bubbles and so the detectors are not capable of precision measurements, but they proved the validity of the technique. In the next phase a few years later (AMANDA-B10), 10 more strings containing 320 optical modules were located at depths between 1.5 and 2.0 km, where the properties of ice are suitable for muon detection. Finally, the current version of the detector (AMANDA-II) has an additional nine strings extending to a depth of 2.35 km. In total there are 680 optical modules covering a cylindrical volume with a cross-sectional diameter of 120 m.

The AMANDA detector has successfully detected atmospheric neutrinos and has produced the most detailed map of the high-energy neutrino sky to date. However, no source of continuous emission has yet been observed that would be a candidate for a point source.

AMANDA can detect neutrinos with energies up to about 10^{15} eV, but an even bigger detector, called IceCube, is under construction at the South Pole. This uses 80 strings each containing 60 optical modules regularly spaced over an area of 1 km^2 at depths of between 1.4 and 2.4 km (the volume covered by AMANDA is only 1.5 per cent of the volume to be covered by IceCube) and will be capable of detecting neutrinos with energies as high as 10^{18} eV. IceCube is due for completion in 2010.

Dark matter

The modern description of the universe is based on the observation that it is expanding and assumes that the origin of this is a sudden explosion at some time in the past. For this reason the description is called the *big bang model*. However, this does not mean an explosion from a singular space–time point. Because the universe appears isotropic at large distance scales, there can be no preferred points in space and so the big bang must have occurred everywhere at once, thus ensuring that the expansion appears the same to all observers irrespective of their locations. Two pieces of evidence for this model are the existence of a cosmic background radiation consistent with a black-body spectrum at an effective temperature of 2.7 K, and the cosmic abundance of light elements.⁵ Whether the expansion will continue indefinitely depends on the average density of the universe ρ . The critical density ρ_c at present times, below which the expansion will continue indefinitely, and above which it will eventually halt and the universe start to contract, can be written

$$\rho_c = \frac{3H_0^2}{8\pi G} \sim 10^{-26} \text{ kg m}^{-3} \approx 5.1 (\text{GeV}/c^2)\text{m}^{-3}, \quad (9.24)$$

where G is the gravitational constant and we have used the best current value for Hubble’s constant H_0 to evaluate Equation (9.24). In the most popular version of the model, called the *inflationary big bang model*, the relative density

$$\Omega \equiv \rho/\rho_c = 1. \quad (9.25)$$

The relative density is conveniently written as the sum of three components,

$$\Omega = \Omega_r + \Omega_m + \Omega_\Lambda, \quad (9.26)$$

where Ω_r is the contribution due to radiation, Ω_m is that due to matter and Ω_Λ is related to a term in the equation governing the evolution of the universe that

⁵For an accessible discussion of the big bang model and other matters discussed in this section see, for example, Pe03.

contains a so-called *cosmological constant* Λ . The latter contribution can be estimated from various cosmological observations, including recently measured temperature fluctuations in the microwave background radiation. Its value is about 0.7 and is the largest contribution to Ω . The value of the radiation term is of the order of 10^{-5} and so makes a negligible contribution to Ω . Finally, the total matter density contribution can be deduced from the gravitational energy needed for consistency with observations on the rotation of galaxies and the kinematics of large-scale structures in the universe. Its value is about 0.3. Thus we see that the value of Ω is consistent with Equation (9.25), although the uncertainties are considerable. An unsatisfactory feature is that the origin of the largest term, also referred to as *dark energy*, is totally unknown.

The contribution of baryons to the mass term may be inferred from knowledge of how nuclei are formed in the universe (*nucleosynthesis*) and its value is about 0.05, of which only about 20 per cent is accounted for in the form of stars, gas and dust, i.e. in the form of visible luminous baryonic matter. There could be other sources of non-luminous baryonic matter, for example in the form of brown dwarfs and small black holes the size of planets, and there is experimental evidence that such ‘massive, compact halo objects’ (MACHOs) do indeed exist, but in unknown quantities. However, it is not thought that they alone can account for the ‘missing’ matter. Thus we are forced to conclude that the bulk of matter, as much as 85 per cent, is non-baryonic. It is referred to collectively as *dark matter*.

There are several dark matter candidates. Massive neutrinos might be one possibility. Such particles would have to be heavy enough to have been non-relativistic in the early stages of the universe (so-called *cold dark matter*), because if they were relativistic (*hot dark matter*) they would have rapidly dispersed, giving rise to a uniform energy distribution in space. Calculations suggest that in this case there would have been insufficient time for the observed galaxies to have formed. Although neutrinos may still play a minor role in contributing to the matter deficit, it is now believed that the bulk of the contribution comes from cold dark matter in the form of ‘weakly interacting massive particles’ (WIMPs). Although there are no known particles that have the required properties, for various reasons the most likely candidates are SUSY particles and in particular the lightest such state, usually taken to be the neutralino.

Experiments such as AMANDA can search for WIMPs, but they were not designed to do so as a priority. However, several dedicated experiments have been mounted to detect WIMPs by detecting the recoil energy of interacting nuclei, which is about 50 keV. Such recoils can, in principle, be detected in a number of ways. For example, in semiconductors such as GaAs, free charge will be produced that can be detected electronically; in a scintillator such as NaI the emission of photons can be detected using photomultipliers; and in crystals at low temperatures the energy can be converted to phonons that can be detected by a very small rise in temperature. In practice, the problems are formidable because of the very low expected event rate. This can be calculated from the expected WIMP velocities and assumed masses. For example, if WIMPs are identified with neutralinos, then

expectations range from 1–10 events per kg of detector per week. This is very small compared with the event rate from naturally occurring radioactivity, including that in the materials of the detectors themselves. The former is minimized by working deep underground to shield the detector from cosmic rays and in areas with geological structures where radioactive rocks are absent; and the latter is minimized by building detectors of extreme purity. Finally, WIMP recoils should exhibit a small seasonal time variation due to the motion of the Earth around the Sun and the motion of the Sun within the galaxy. One experiment claims to have seen this variation. Present experiments are at an early stage, but some versions of SUSY theories with low-mass neutralinos can probably already be ruled out.⁶

Matter–antimatter asymmetry

One of the most striking facts about the universe is the paucity of antimatter compared with matter. There is ample evidence for this. For example, cosmic rays are overwhelmingly composed of matter and what little antimatter is present is compatible with its production in intergalactic collisions of matter with photons. Neither do we see intense outbursts of electromagnetic radiation that would accompany the annihilation of clouds of matter with similar clouds of antimatter. The absence of antimatter is completely unexpected because, in the original big bang, it would be natural to assume a total baryon number $B = 0$.⁷ Then during the period when kT was large compared with hadron energies, baryons and antibaryons would be in equilibrium with photons via reversible reactions such as



and this situation would continue until the temperature fell to a point where the photons no longer had sufficient energy to produce $p\bar{p}$ pairs and the expansion had proceeded to a point where the density of protons and antiprotons was such that their mutual annihilation became increasingly unlikely. The critical temperature is $kT \approx 20$ MeV and at this point the ratios of baryons and antibaryons to photons ‘freezes’ to values that can be calculated to be

$$N_B/N_\gamma = N_{\bar{B}}/N_\gamma \sim 10^{-18}, \quad (9.28)$$

⁶An up-to-date review of the status of dark matter searches is given in Pe03 and Ei04.

⁷One could of course simply bypass the problem by arbitrarily assigning an initial non-zero baryon number to the universe, but it would have to be exceedingly large to accommodate the observed asymmetry, as well as being an unaesthetic solution.

with of course $N_{\bar{B}}/N_B = 1$. These ratios would then be maintained in time, whereas the actual observed ratios are

$$N_B/N_\gamma \approx 10^{-9}, \quad N_{\bar{B}}/N_\gamma \sim 10^{-13}, \quad (9.29)$$

with $N_{\bar{B}}/N_B \sim 10^{-4}$. The simple big bang model fails spectacularly.

The conditions whereby a baryon–antibaryon asymmetry could arise were first stated by Sakharov. It is necessary to have: (a) an interaction that violates baryon number conservation, (b) an interaction that violates charge conjugation, and (c) a non-equilibrium situation must exist at some point to ‘seed’ the process. We have seen in Chapter 6 that there is evidence that CP is violated in the decays of some neutral mesons, but its source and size are not compatible with that required for the observed baryon–antibaryon asymmetry and we must conclude that there is another, as yet unknown, source of CP violation. Likewise a method for generating a non-equilibrium situation is also unknown, although it may be that the baryon-violating interactions of GUTs, which are necessary for condition (a), may provide one. Clearly, matter–antimatter asymmetry remains a serious unsolved problem.

9.2 Nuclear Physics

Despite more than a century of research, nuclear physics is by no means a ‘closed’ subject. Even the basic strong nucleon–nucleon force is not fully understood at a phenomenological level, let alone in terms of the fundamental quark–gluon strong interaction. Indeed one of the outstanding problems of nuclear physics is to understand how models of interacting nucleons and mesons arise as approximations to the quark–gluon picture of QCD and where these two descriptions merge. A related question is whether the nuclear environment modifies the quark–gluon structure of nucleons and mesons. It follows from our lack of knowledge in these areas that the properties of nuclei cannot at present be calculated from first principles, although some progress has been made in this direction. Meanwhile, in the absence of a fundamental theory to describe the nuclear force, we have seen in earlier chapters that specific models and theories are used to interpret the phenomena in different areas of nuclear physics. Current nuclear physics models must break down at very high energy-densities and at sufficiently high temperatures the distinction between individual nucleons in a nucleus should disappear. This is the regime that is believed to have existed in the very early times of the universe and is of great interest to astrophysicists.

Nuclear physics is a mature subject and has implications in many other areas of physics and wide applications in industry, biology and medicine that are at the core of the subject. Examples include: the nuclear physics input required to understand many processes that occur in cosmology and astrophysics, such as supernovae and

the production of chemical elements; the many applications of NMR, such as studies of protein structure and its use in medical diagnostics; and industrial applications such as the production of power. In Chapter 8 we touched on just three applications and the ‘applied’ problems to be solved in those – safe disposal of nuclear waste, better medical imaging diagnostics and therapeutics, controlled nuclear fusion, etc. – are as demanding as the ‘fundamental’ ones, simply different. They are also vitally important for the future well-being of everyone. In the sections that follow we will take a brief look at a few of these pure and applied problems.⁸

9.2.1 The structure of hadrons and nuclei

In the standard model, the structure of nucleons is specified in terms of quarks and gluons, but questions remain. One concerns the spin of the proton. This must be formed from combining the spins and the relative orbital angular momenta of its constituent quarks and gluons. Measuring these various contributions can be done in deep inelastic scattering experiments of the type described in Chapter 5, but using spin-polarized targets, sometimes with spin-polarized beams. Experiments to date have shown the surprising result that the spins of all the quarks and antiquarks together contribute only about 20–30 per cent to the total spin of the proton (the so-called ‘proton spin crisis’). There is some information that the angular momentum contributions of the quarks play an important role, but very little is known about the contribution of the total angular momentum of the gluon. This is an area where the type of experiment that can be pursued at the CEBAF accelerator described in Section 4.2.2 will be vital in unravelling the details of each contribution and thus further testing QCD.

Nucleons and mesons are the building blocks of nuclear matter, but there is no guarantee that the properties of these particles in nuclei are identical to those exhibited as free particles. According to QCD the properties of hadrons are strongly influenced by the sea of quark–antiquark pairs and gluons that we have seen in Chapter 5 are always present around confined quarks due to quantum fluctuations. However, these influences could well be different in the case of closely spaced nucleons in nuclear matter from those for a free nucleon. Indeed there are theoretical predictions that the probability of finding a $q\bar{q}$ pair decreases as the density of the surrounding nuclear matter increases. If such effects could be established they would have a profound influence on our understanding of quark confinement.

⁸A comprehensive overview of the field as at 1999 is a report of the Board on Physics and Astronomy of the National Research Council, USA: “*Nuclear Physics: The Core of Matter, The Fuel of Stars*”, National Academy Press, Washington, D.C. (1999) – NRC99. Other useful sources are the publications of the Nuclear Physics European Collaboration Committee (NuPecc) and in particular its “*Report on Impact, Applications, Interactions of Nuclear Science*” (2002) and the NuPecc Long-Range Plan 2004.

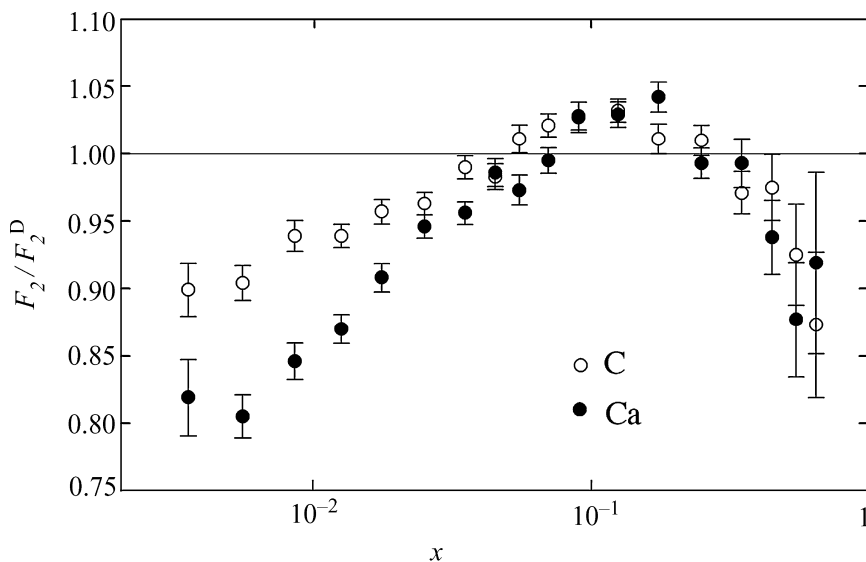


Figure 9.9 The ratios of the F_2 structure function found from nuclear targets to that found from deuterium, as a function of the scaling variable x (Carbon data from Ar95, calcium data from Am95)

Another consequence of these predictions is that the effective masses of hadrons will in general change in nuclear matter, as will their sizes and interactions. There is already some evidence in favour of this suggestion from deep inelastic scattering from nucleons (see Section 5.7) where the structure functions obtained using targets of light and heavier nuclei differ slightly, even after allowing for calculable effects such as nuclear binding energies and the internal Fermi motion of the nucleons. (This is the so-called ‘EMC effect’, named after the group that first discovered it.) It is illustrated in Figure 9.9, which shows the ratios $F_2^{\text{Ca}}/F_2^{\text{D}}$ and $F_2^{\text{C}}/F_2^{\text{D}}$, i.e. the F_2 nucleon structure function deduced from calcium and carbon targets divided by the structure function deduced using a deuterium target.

A number of other experiments have been performed to detect the effect of the nuclear environment on effective masses (for example, by determining the mass of mesons produced in nuclear matter) but nothing significant has been found elsewhere. This will be a continuing field of study.

It is also important to study how the interactions of lower-energy hadrons change when they are embedded in nuclear matter. For example, there is considerable interest in the interactions of hadrons containing a strange valence quark. (One reason is that they may play an important role in the high-density matter present in neutron stars.) The lightest mesons that contain a strange valence quark or antiquark are the kaons and these can be implanted in nuclei by nuclear reactions that substitute a strange quark for an up or down quark. (This is an example of a so-called ‘hypernucleus’.) Experiments at CEBAF and other

laboratories will provide information on the interaction of implanted, negatively charged kaons with the surrounding nucleons in a nucleus.

The facilities at CEBAF and RHIC (the relativistic heavy ion accelerator described in Section 4.2.2) will enable a range of new experimental possibilities to be explored, in addition to those above. One is the intriguing question of the existence of glueballs (mesons made of gluons alone) and hybrid quark–gluon mesons, mentioned in Section 5.2 and vital for the theory of confinement via QCD. The results may well help to find a solution to one of the central questions posed at the start of this section: how are the properties of the strong nuclear force related to the standard model formulation in terms of quarks and gluons?

There are also questions to be answered in the realm of nuclear structure, many with implications elsewhere. For example, can the properties of nuclei be related to those of an underlying nucleon–nucleon interaction and can they be derived from many-body theory? At present we have a good knowledge from scattering experiments of the long-range part of the nucleon–nucleon force in terms of meson exchanges (see Section 7.1), but models that fit data differ about the short-range part. This is not surprising because at separations of less than 1 fm a description in terms of quarks and gluons is necessary and the interface with QCD is critical. Experiments on meson production in nucleon–nucleon collisions are sensitive to the short-range part of the forces and should provide information on this region. On the theoretical side, advances in computer power and calculational techniques have enabled the binding energies of all light nuclei to be successfully calculated using the best available parameterization of the nucleon–nucleon force. However, this is only possible by including an explicit weaker three-nucleon force, which has to be adjusted to obtain the correct binding energies. A satisfactory theory of the three-body force between nucleons is lacking. This work also needs to be extended to heavier nuclei, but present computer power is inadequate to the task using current computational techniques.

One approach to the latter problem is to work within the framework of the shell model, where each nucleon moves in the average potential (the mean field) generated by its interactions with all the other nucleons in the nucleus. We have seen the successes of this approach in simple applications in Section 7.3. When combined with further computational improvements, it has enabled nuclear structure calculations to be extended to $A = 56$. This is an important point for astrophysics, because the details of the nuclear reactions of iron control the critical process occurring in the collapse of a supernova, as we have seen above in Section 9.1.4.

Very often in science new insights are achieved by pushing experiments to their limits. Nuclear physics is no exception. One such limit is the quest for super-heavy elements. Discovery of elements beyond those currently known could explore questions about possible limits on nuclear charges and masses. According to nuclear models there should exist a new group of super-heavy elements with charges Z in the range approximately 114 to 126 that are stabilized by shell effects.

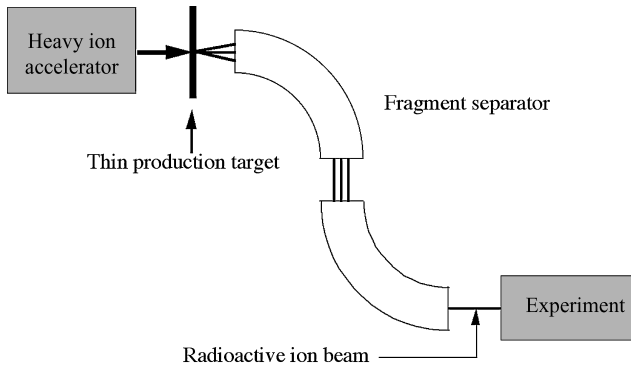


Figure 9.10 An energetic particle (typically several tens of MeV/u to GeV/u) is fragmented in a nuclear reaction in a thin target, and radioactive reaction products are separated in-flight and transported as a secondary beam to the experiment

The heaviest element made to date has $Z = 116$ and was produced by fusion in the reaction ${}^{48}_{20}\text{Ca} + {}^{248}_{96}\text{Cm} \rightarrow {}^{292}_{116}\text{Uuh} + 4n$ (the symbol Uuh is used as the element has yet to be named). Strenuous efforts are being made to reach the predicted new island of relative stability. This will require facilities to produce exotic short-lived nuclear beams and there is much development work going on in this area. One example of how such a beam can be formed is shown in Figure 9.10. The other main method employs two independent accelerators: a high-power driver accelerator for production of the short-lived nuclei in a thick target that is directly connected to an ion-source, and a second post-accelerator. Radioactive atoms diffuse out of a hot target into an ion source where they are ionized for acceleration in the post-accelerator.

Fewer than 300 stable nuclei occur naturally (see Figure 2.7) and outside the stability region nuclei decay by the mechanisms discussed in Chapters 2 and 7. In the uncharted regions there are many fundamental questions to be answered, such as what are the limiting conditions under which nuclei can remain bound and do new structures emerge near these limits? The answers to these questions are important because theoretical descriptions of nuclei far from the line of stability suggest that their structures are different from what has been seen in stable nuclei. Nuclei far from stability also play an important role in astrophysics, for example in understanding the processes in supernovae and how elements are synthesized in stars. Another limiting region that is expected to yield interesting information is that of angular momentum. Super-deformed nuclei have been discovered with highly elongated shapes and very rapid rotational motion. The states associated with these shapes are extremely stable. Further investigation of these is expected to yield important information about nuclear structure.

9.2.2 Quark–gluon plasma, astrophysics and cosmology

We have touched on the implications of nuclear physics for astronomy at various places above. Here we look at other areas where improvements in our nuclear physics knowledge would help astrophysics and cosmology.

In QCD, quarks and gluons are confined within hadrons, although the nature of this confinement is still not fully understood. At extremely high energy-densities the quarks and gluons are expected to become deconfined across a volume that is large compared with that of a hadron. They would then exist in a new state of matter, called a *quark–gluon plasma*, which is the state of nuclear matter believed to have existed in the first few microseconds after the big bang (see Figure 9.11).

It is possible to probe this state of matter using the RHIC facility (and also in a few years at the LHC when its construction is complete). RHIC typically collides two counter-circulating beams of fully-stripped gold ions at a maximum energy of 200 GeV per nucleon. If the ions collide centrally (i.e. head-on) several thousand final-state particles are produced. An example of an event seen in the STAR detector (which was shown in Figure 4.20) is illustrated in Figure 9.12. A key

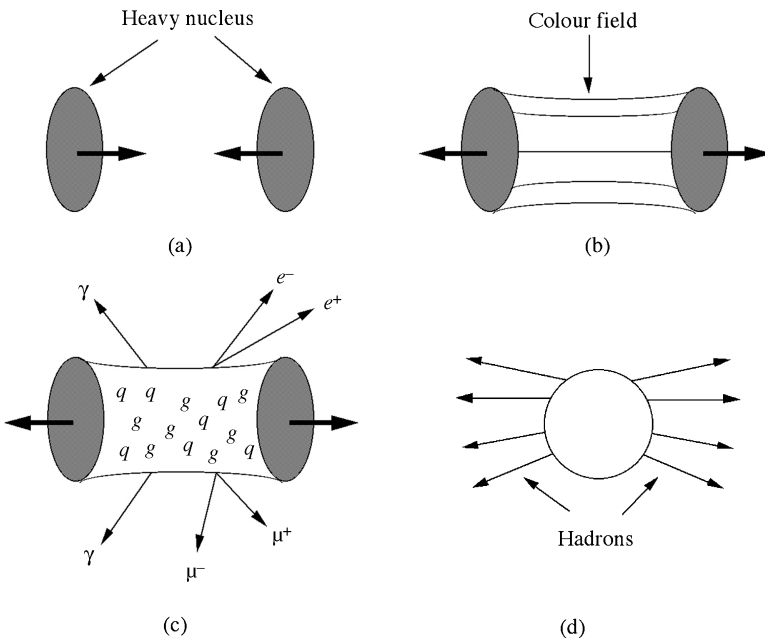


Figure 9.11 Stages in the formation of a quark–gluon plasma and subsequent hadron emission: two heavy nuclei collide at high energies (a) and interact via the colour field (b); the very high energy-density produced causes the quarks and gluons to deconfine and form a plasma that can radiate photons and lepton pairs (c); finally, as the plasma cools, hadrons condense and are emitted (d) (after NRC99, with permission of the National Academics Press)

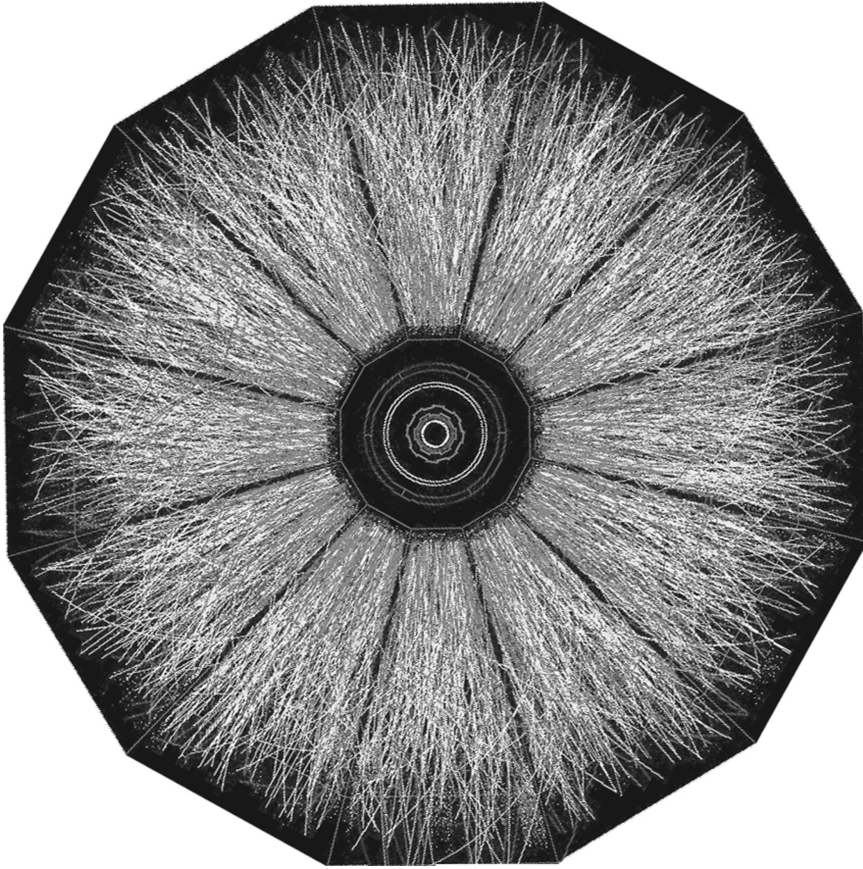


Figure 9.12 View of a 200 GeV gold–gold interaction in the STAR detector at the RHIC accelerator (Courtesy of Brookhaven National Laboratory)

question is whether the energy-density in the collisions is sufficient to have created a quark–gluon plasma and its subsequent cooling phases. There are many signatures for this, including the relative abundances of different final-state particle types (for example, production of the $c\bar{c}$ meson J/Ψ would be suppressed) and measurements are all consistent with the expected temperature at which hadrons would be formed (about 176 MeV, corresponding to about 10^{12} K, close to that predicted by QCD) and that the temperature of the initial fireball is considerably higher.

Future experiments at RHIC will play a crucial role in understanding the basic nature of deconfinement. Questions to be addressed include: what is the nature of matter at the highest densities (very recent experiments at RHIC suggest that the plasma behaves more like a liquid than a gas); under what conditions can a quark–gluon plasma be made; and what are the rules governing the evolution and the transition to and from this kind of matter?

Information gathered from high-energy heavy-ion collisions is potentially important in astrophysics. It will help constrain the equation of state that relates the density of matter in neutron stars and supernovae (as well as in the first microseconds of the early universe) to pressure and temperature. This information will place stronger theoretical constraints on the maximum mass of a neutron star, improving the ability to distinguish neutron stars and black holes.

The synthesis of nuclei in the very early universe is one of the cornerstones of modern astrophysics, but even here there are still surprises. For example, in the discussion of stellar fusion in Chapter 8, we saw that the production of heavy elements involves the rare reaction $3(^4\text{He}) \rightarrow ^{12}\text{C}$ (Equation (8.31)), the occurrence of which depends critically on the existence of a particular excited state of ^{12}C . We also noted that very recently another excited state has been discovered at a somewhat higher energy which has the effect of significantly altering the energy dependence (or equivalently the temperature dependence) of this reaction from the values usually assumed. This could have major consequences for models and theories of stellar evolution. Another recent experiment has measured for the first time the lifetime of the doubly-magic nucleus ^{78}Ni and finds it to be shorter than expected, implying that supernova explosions may produce gold and other heavier elements much faster than had previously been thought. This is important because ^{78}Ni is believed to produce more than half the elements heavier than iron in the universe. A reaction of great current interest is the synthesis of ^{16}O from the reaction of ^4He with ^{12}C (Equation (8.32)), which determines the relative sizes of the carbon and oxygen shells of massive stars that later explode in supernovae. The sizes of these shells are a crucial factor in predicting the nucleosynthesis that occurs during the explosion. Nuclear physicists are currently trying to measure the rate of this reaction with sufficient accuracy to constrain astrophysical models.

One of the outstanding theoretical challenges in nuclear astrophysics is to understand the process by which a massive, fully-evolved star ejects its mantle while its core collapses to a neutron star or black hole. In Section 9.1.4 above we gave a simple description of this process involving the collapse of the iron core to several times the density of nuclear-matter, thereby producing a powerful shock wave that travels outward through the mantle of the star. This shock wave, aided by the heating of the matter by neutrinos emitted by the newly formed neutron star, is responsible for the ejection of the mantle. This is the broad-brush picture, but there is still no satisfactory theory that can account for the observed frequency of supernovae. Efforts to understand dense nuclear matter and to predict the properties of neutron stars depend on knowledge of nuclear interactions gained in the laboratory. Heavy-ion collisions will help us better understand the interactions of mesons in hot, dense nuclear matter, which is crucial to the issue of meson condensation in neutron stars. Future studies of neutron-rich nuclei, near the limit of stability, in radioactive ion beam facilities, as mentioned in Section 9.2.1 above, will allow more accurate modelling of nuclear forces in neutron star crusts.

9.2.3 Symmetries and the standard model

An important symmetry that can be tested in nuclear physics is time reversal. We have seen in Section 6.6 that CP invariance is violated in the weak decays of K and B mesons and by inference so is T invariance, provided CPT invariance holds. However, we have also seen in Section 9.1.4 above that the mechanism of violation that can explain meson decays is unable to explain the observed matter/antimatter asymmetry in the universe. Thus it is likely there exists another CP -violating mechanism and hence another source of T violation.

There are several ways in principle of exploring CP violation in the context of atomic and nuclear physics. One way involves antihydrogen. This was first produced in a controlled experiment in 2002 by mixing cold antiprotons with a dense positron plasma confined by electromagnetic fields in a so-called ‘Penning trap’. If atoms of antihydrogen could be trapped for extended periods their properties could be compared with those of hydrogen and this might shed light on matter–antimatter asymmetry. CP violation can also be probed by searching for electric dipole moments (EDMs) of the neutron, atoms or the electron. In the case of atoms, an EDM could arise if the electron had an electric dipole moment or if there were a T -violating interaction within the nucleus. Static EDMs are forbidden if T invariance is exact and so a non-zero value would imply CP violation, assuming CPT invariance holds. The present 90 per cent confidence limit on the EDM d_n of the neutron is $d_n < 6.3 \times 10^{-26}$ e cm and that for the electron is $d_e < 1.6 \times 10^{-27}$ e cm. Improving these presents formidable experimental challenges. Nevertheless, several experiments are planned or are underway to measure EDMs, with the aim of reducing the bounds to regions where they could test the predictions of current theories. For the standard model these are $d_n \sim 10^{-31}$ e cm and $d_e \sim 10^{-38}$ e cm, although some extensions of the standard model discussed in Section 9.1.3 above predict considerably larger values. Limits on the existence of atomic and neutron EDMs already provide constraints on some of the most plausible extensions to the standard model. It is also possible that T -violation might show up in the decay of an unstable system. Modern experiments are searching for T -violating correlations in the β -decay of neutrons, mesons and particular nuclei.

Atomic/nuclear physics can also provide information on the standard model in other areas of the weak interactions. For example, a recent (2005) study of the β -decay of a metastable state of ^{38}K in an atomic trap has enabled severe limits to be placed on a possible spin-0 particle to augment the spin-1 W -meson exchange. The mixing between the weak and electromagnetic interactions can also be studied. This is characterized by the Weinberg angle, which can be measured in the parity-violating interaction between electrons and the nuclei of particular atoms. This was mentioned at the end of Section 6.7. Parity mixing has been seen in several atomic systems. The best measurement at present has been made using ^{133}Cs atoms, although the limits on the Weinberg angle do not yet compete with

those obtained from particle physics experiments. Other experiments plan to study this effect in atomic francium, where the parity-mixing effect should be about 18 times larger. (The effect of an electric dipole moment of the electron is also expected to be greatly enhanced in francium.) Unfortunately, francium is an extremely rare element with no stable isotopes and so experiments will be carried out with a small number of radioactive atoms collected in a magneto-optic trap.

9.2.4 Nuclear medicine

In Section 8.3.1, we reviewed the use of radiation techniques for cancer therapy. We also briefly mentioned that in principle heavier particles had advantages over photons. For example, because of the form of the Bragg curve, protons deposit more of their energy where they stop, not where they enter the body. Also their depth of penetration can be precisely controlled so that they stop within the tumour, thus allowing radiologists to increase the radiation dose to the tumour while reducing the dose to healthy tissues.

This is illustrated in Figure 9.13, which compares the treatment plans (i.e. simulations of the pattern of radiation that the patient would receive) for treating a case of advanced pancreatic cancer. Figure 9.13(a) shows an X-ray plan using a ‘state-of-the-art’ nine-beam X-ray system. The amount of radiation received by nearby organs and other critical areas (kidneys, liver and spinal chord) is seen to be a substantial fraction of the dose received by the region of the cancer. This is contrasted with the results of Figure 9.13(b), which is for treatment using a single proton beam. Although there is some unwanted exposure at the input site

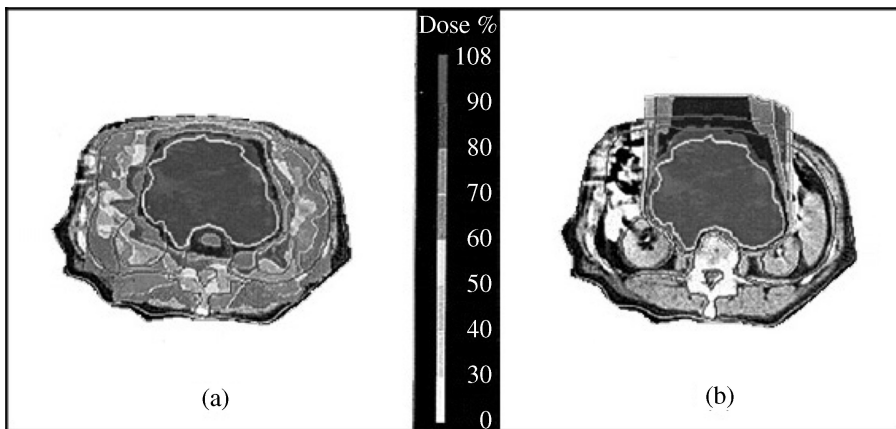


Figure 9.13 Treatment plans for a large pancreatic tumour: (a) using a nine-beam X-ray system; (b) using a single proton beam. The diffuse grey areas in (a) indicate the spread of energy deposition outside the region of the tumour (adapted from Zu00, copyright Elsevier, with permission)

(which could be lessened by a system of multiple beams or a rotating beam), the radiation energy is concentrated much more within the area of the tumour.

Although they have great potential, the problem with using particle beams is the practical one of access to suitable accelerators. There is considerable effort being made to design proton accelerators for cancer therapy and more than 20 centres now exist worldwide specifically for proton therapy. Research is also continuing with other forms of radiation therapy using neutrons and heavy ions. Neutrons produce a high linear energy transfer (LET) and this overcomes a cancer cell's resistance to radiation damage more effectively than low-LET photon, electron or proton radiation. Thus neutrons appear to be more biologically effective in killing cancers than many other forms of radiation, especially in oxygen-poor cells. Beams of heavy ions, such as carbon or neon, with energies of 400–800 MeV per nucleon, are nearly ideal dose delivery vehicles for radiation therapy. Limited studies with carbon and neon beams have been conducted and doubtless these studies will increase in the future.

Progress in the NMR technique in medicine continues. For example, recent advances have enabled a variation known as functional MRI (fMRI) to be developed that exploits the paramagnetic behavior of deoxyhaemoglobin in red blood cells. When in a magnetic field, a blood vessel containing deoxyhaemoglobin distorts the field in its immediate environs, with the degree of distortion increasing with the concentration of deoxyhaemoglobin. This distortion affects the behaviour of water protons in the environs and, consequently, the magnetic-resonance signal arising from these protons. Neural activation of a region of the brain stimulates increased arterial flow of oxygenated blood, thereby decreasing the concentration of deoxyhemoglobin in the region. Changes in the magnetic-resonance signal can be detected and displayed as functional-MRI images. These so-called BOLD (blood-oxygen-level dependent) images enable studies to be made of the way the brain works by taking MRI images in real time while the patient is performing specific tasks. In this way areas of the brain can be studied that are associated with particular activities or sensations.

As another example, the gases ^3He and ^{129}Xe have the magnetic properties needed for MRI and the atomic structure needed to retain their polarization for hours at a time. They can be introduced into lungs, allowing MRI studies of lung function. Because of the strong signal provided by the polarized nuclei in the gas atoms, the MRI scans are short and can be synchronized with breathing. Developments are also being made towards general high-speed imaging, which would be useful for claustrophobic patients and children who are unable to be in the confined environment of a conventional MRI magnet for sometimes up to an hour.

Perhaps the greatest potential of all lies in the imaging of nuclei other than hydrogen, particularly the phosphorus nucleus. Phosphorus is a major constituent of the molecules adenosine triphosphate (ATP) and phosphocreatine, which mediate the transfer of energy in living cells. From knowledge of such concentrations it is possible to infer the metabolic status of internal organs, and it may

eventually be possible to add this capability to an imaging instrument. The future will undoubtedly see both an improvement in the quality of NMR images and a growing diversity of applications for nuclear magnetic resonance in clinical practice.

An area that was not mentioned in Chapter 8 is the use of radioactive nuclear isotopes produced by accelerators or nuclear reactors in many areas of biological and biomedical research. For example, by inserting such radioisotopes as ^{14}C and tritium, it is possible to obtain information on how molecules move through the body, what types of cells contain receptors, and what kinds of compounds bind to these receptors. Radioisotopes are also used directly to treat disease and radioactive tracers are indispensable tools for the new forensic technique of DNA fingerprinting, as well as for the Human Genome Project.

9.2.5 Power production and nuclear waste

Nuclear fusion still holds the promise of unlimited power without the problem of radioactive waste, but the road to realization of this goal is long and we are far from the end. In Section 8.2 we introduced the Lawson criterion as a measure of how close a design was to the ignition point, i.e. the point at which a fusion reaction becomes self-sustaining. To date no device has yet succeeded in achieving the Lawson criterion and much work remains to be done on this important problem. In recognition of this, at least one major new tokamak machine (to be built in France) is planned as a global collaboration, but even when the ignition point is attained, based on experience with fission reactors, it could be many decades before that achievement is translated into a practical power plant.

In the shorter term and assuming that renewable sources of energy are insufficient to fulfil the world's increasing energy needs, it does seem as if power plants based on fission reactions are the only hope of replacing fossil fuels in the future. The problems of reactor safety and the safe disposal of radioactive waste are therefore paramount.

The waste from light-water reactors, the most common type of power reactor, has two major components: the actinides, i.e. any of the series of radioactive elements with atomic numbers between 89 and 103 (mainly uranium but also smaller amounts of heavier elements, the transuranic elements like plutonium and the minor actinides such as neptunium, americium and curium) and fission products, which are medium-weight elements from fission processes in the nuclear fuel. While it is generally agreed that radioactive nuclei with relatively short lifetimes can be safely stored in deep geological disposal facilities, the same is not true of waste with very long lifetimes, some of which are water-soluble and so have the potential to contaminate ground water. An additional problem is the disposal of material that could be used for nuclear weapons, i.e. ^{239}Pu and ^{235}U . One option for handling waste with very long lifetimes, which was mentioned as a theoretical possibility in Section 8.1.3, is to transmute it by neutron reactions into

shorter-lived, or even stable, isotopes that can be dealt with by conventional storage.

The idea of using an accelerator to produce materials that can only be made artificially has been around for more than 40 years, but more recently there has been considerable interest and research in this idea to ‘incinerate’ nuclear waste with the aim of reducing the waste lifetimes to less than 100 years. This is referred to as ADS – Accelerator Driven System. In one proposed scheme, uranium and most of the plutonium would be separated prior to proton irradiation and used again as reactor fuel. The most important long-lived components of the remaining waste would be isotopes of neptunium, americium, curium and iodine, some with half-lives of 10 000 years or more. The approach would be to irradiate this material with a new source of fast neutrons produced by spallation reactions (cf. the discussion of producing neutron beams by this process in Section 4.2.3) initiated using protons from a high-current accelerator. In this way the capacity to ‘burn’ long-lived fission products and actinides is greatly increased, leaving waste with much shorter lifetimes which can be disposed of by conventional means. The accelerator would deliver a high-power (10–20 mA) proton beam of about 1 GeV energy to a heavy metal (spallation) target surrounded by the nuclear waste to be incinerated. The accelerator–waste combination would be operated at a subcritical level – by itself it could not sustain a chain reaction – so that no reactor-core meltdown accident could occur.

It has been suggested that this concept might be carried one step further, and a particle beam might be used to produce additional neutrons directly in a nuclear-reactor-like core. Versions of this concept have been studied in America and by a European group. The latter is based on a proposal by Rubbia⁹ and is called the Energy Amplifier. In this scheme, the core of the reactor would again be subcritical, and the accelerator beams would provide sufficient additional neutrons via the spallation reaction to run the reactor. An idealized possible set-up is shown in Figure 9.14.

Because the spallation neutrons would have high energy, a less enriched element, such as natural thorium, could serve as the fuel. Thorium has the great advantage over uranium in being an abundant element that does not require costly isotope separation. Although the thorium fuel would not require enrichment, it would need to be recharged every 5 years or so. The proposal has a number of other advantages over a conventional power reactor, including: it is sub-critical without the spallation neutrons and so is inherently safe – a meltdown or explosion is not possible; radioactive waste is consumed in the reactor and no long-lived waste is produced; there is no overlap with the nuclear weapons fuel cycle and so the energy amplifier cannot be used as the basis for producing materials for nuclear weapons, making installations politically acceptable worldwide.

⁹The same man who shared the 1984 Nobel Prize in Physics for the discovery of the *W* and *Z* bosons.

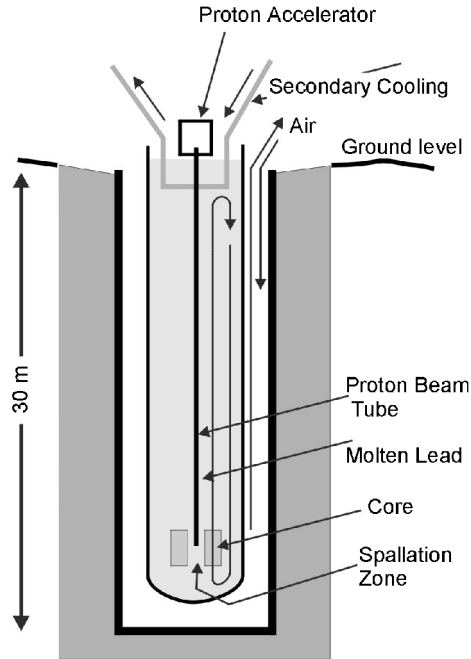


Figure 9.14 Schematic diagram of a possible configuration of an energy amplifier; in this design the coolant and spallation metal is molten lead (from Sc01, copyright Cavendish Press Ann Arbor 2001, with permission)

The possible energy flow in a commercial system is shown in Figure 9.15. This assumes a 1 GeV, 20 ma proton beam requiring about 20 MW of input power. The latter is taken from the output of the reactor leaving a net electrical output of 580 MW, i.e. a gain factor of about 30.

The current situation on the energy amplifier is that a European collaboration has shown that initial partitioning at the level of 95–99 per cent is possible

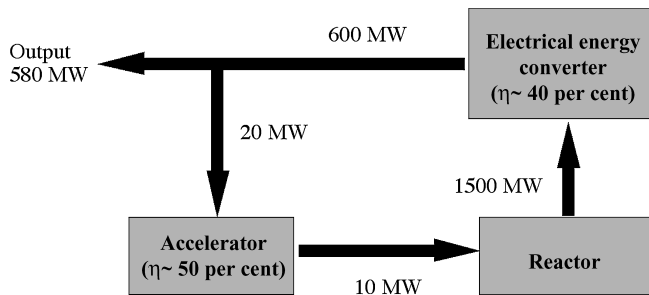


Figure 9.15 Possible energy flows in an energy amplifier system; the conversion efficiencies are denoted by η

depending on the actinide species. They have also carried out a number of successful reactor transmutation and spallation studies and the first full ADS experiment (TRADE) is currently under construction. This consists of coupling a cyclotron delivering a 140 MeV, 0.5–1.0 ma proton beam to an existing 1MW water-cooled reactor sited in Italy and uses a spallation target of tantalum. The operation date is planned for 2007/08. Additional work is being carried out in Belgium on coupling a 350 MeV, 5 ma proton beam to a 100 MW subcritical reactor (the Myrrha experiment) and has already shown that some long-lived isotopes can be successfully incinerated. Although ADS has enormous potential, there are still a great many problems to be overcome and questions to be answered. The estimated time for completion of research and development work and commencement of an industrial plant based on ADS could be as long as 50 years.